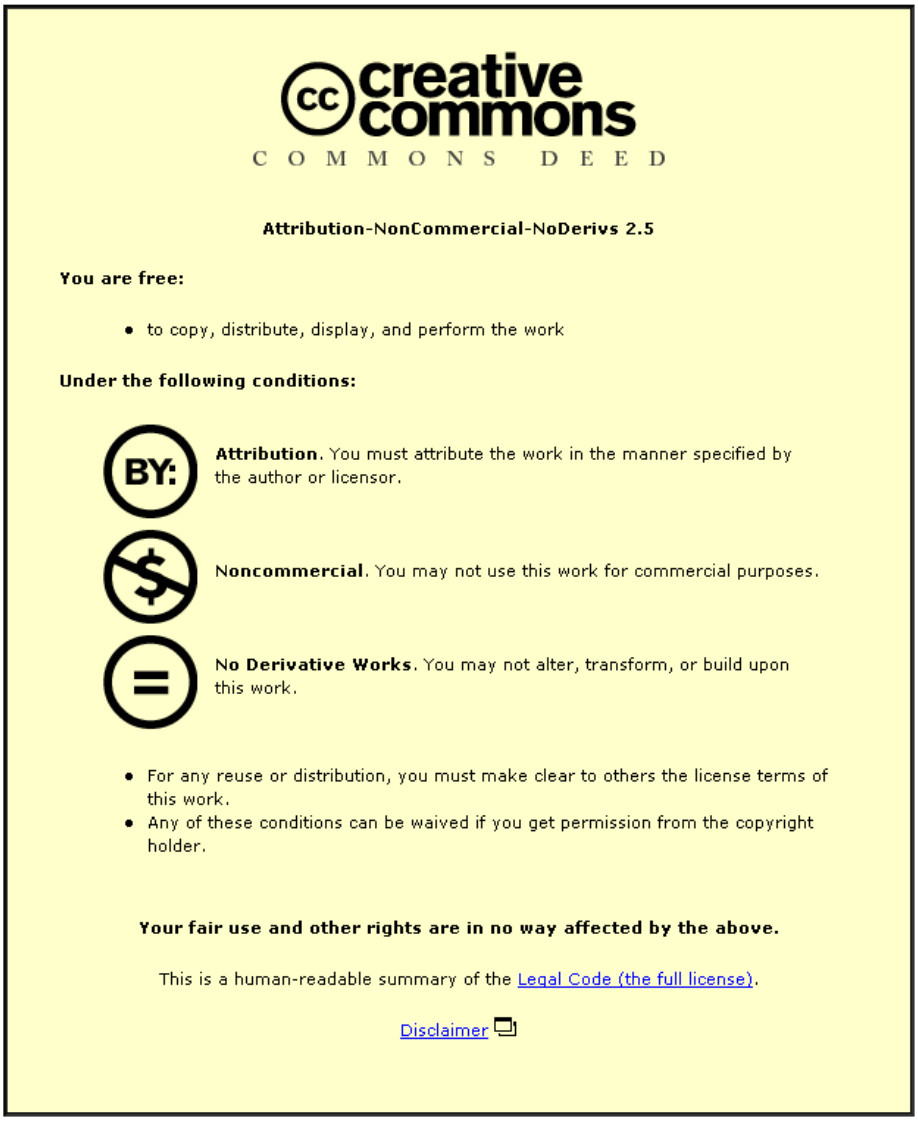

creative commons

COMMONS DEED

Attribution-NonCommercial-NoDerivs 2.5

You are free:

- to copy, distribute, display, and perform the work

Under the following conditions:

Attribution. You must attribute the work in the manner specified by the author or licensor.

Noncommercial. You may not use this work for commercial purposes.

No Derivative Works. You may not alter, transform, or build upon this work.

- For any reuse or distribution, you must make clear to others the license terms of this work.
- Any of these conditions can be waived if you get permission from the copyright holder.

Your fair use and other rights are in no way affected by the above.

This is a human-readable summary of the Legal Code (the full license).

Disclaimer

Evaluation of the reliability of the measurement of key magnetocaloric properties: A Round Robin study of La(Fe,Si,Mn)H_δ conducted by the SSEEC consortium of European laboratories

K. Morrison*, K.G. Sandeman and L.F. Cohen

The Blackett Laboratory, Imperial College, London SW7 2BZ, UK

C.P. Sasso and V. Basso

Istituto Nazionale di Ricerca Metrologica, Strada delle Cacce 91, 10135 Torino, Italy

A. Barcza, M. Katter

Vacuumschmelze GmbH & Co. KG, Grüner Weg 37, 63450 Hanau, Germany

J.D. Moore, K.P. Skokov and O. Gutfleisch

Leibniz Institute of Solid State and Materials Research (IFW Dresden), PO Box 260016 D-01171, Dresden, Germany

*Corresponding author: Tel: (+44) 207 594 7563, E-mail: kelly.morrison02@imperial.ac.uk,

Abstract

Managing refrigeration of our homes, our food and our work environments in energy efficient ways is of increasing importance. Refrigeration using solid state magnetic cooling is one of a number of technologies that may make a significant contribution to addressing this problem. In order to develop materials that may enable commercial development of this increasingly relevant field it is important to review the reliability of methods used to extract key physical properties, so that as the field matures the community can develop recognised standards of measurement. Here we measure key physical properties in one composition taken from a series of La(Fe,Si,Mn)H_δ 1:13-type samples grown by a source laboratory and measured independently in a consortium of European laboratories using both commercial and bespoke facilities.

Keywords: Demagnetization, magnetic refrigerator, magnetic property, standardization

1. Introduction

The magnetocaloric effect (MCE) is the change in temperature (ΔT_{ad}) of a magnetic material caused by applying a magnetic field (H). The effect is greatest at temperatures near a magnetic phase transition such as a paramagnetic (PM) to ferromagnetic transition (FM) where large changes in the magnetisation (M) take place. It is known as the giant magnetocaloric effect (GMCE) when a first order coupled magneto-structural or magneto-elastic transformation takes place. Indeed, the discovery of GMCE in $Gd_5(Si_2Ge_2)$ (Pecharsky and Gschneidner 1997[a]), initiated intense research activity (Gschneidner and Pecharsky 2000; Tegus et al. 2002) and the MCE has received growing interest more widely due to its potential use for environmentally friendly and energy efficient solid state magnetic cooling at room temperature (Gschneidner 2005, Gutfleisch 2011; Sandeman 2011; Tassou et al. 2010).

The current challenge from a materials perspective lies in finding a magnetic refrigerant with large isothermal entropy change (ΔS) that can be implemented in a cooling process. There are several key physical properties that have to be optimised in order to make a potentially useful material. The balance between magnitude of the ΔS and thermal and magnetic hysteresis (ΔH) that result from materials which show first order character; the resulting adiabatic temperature change, $\Delta T_{ad,}$ which is limited by the absolute magnitude of the heat capacity, C_p, (Gschneidner et al. 2005); and finally the magnitude of the magnetic field required to induce the transition which should be as small as possible due to the expense associated with producing rare earth permanent magnets (Humphries 2010; Schüler et al. 2011). The $La(Fe_xSi_{1-x})_{13}$ system appears to offer a unique combination of characteristics with large ΔS of up to $30 JK^{-1}kg^{-1}$ in field changes of 0-5 T, coupled with remarkably small hysteresis, ΔH, and a T_c easily tuneable by interstitial addition of H (Fujita et al. 2003; Lyubina et al. 2008), or by doping with Co (Hu et al. 2005; Lyubina et al. 2008). Other advantages are cheap and abundant raw materials and easy preparation (Yan et al. 2005)

As the field grows the community is faced with a specific problem related to the reliability of measurement of the key physical properties M, ΔS, C_p and ΔT_{ad}. In order to address this problem we have conducted a round robin exercise, passing a series of La(Fe,Si,Mn)H_δ samples between four European laboratories (denoted here as IC, INRIM, VAC, and IFW – see contributing institutions in author list), equipped with different commercial and bespoke measurement facilities in order to examine variability of measurement and analysis methods and the resulting measurements. We find that absolute agreement between measurements is quite a challenge, primarily due to variation in sample shape and measurement protocols used in different laboratories. Most notably commercial instrumentation can lead to the greatest discrepancies. The work highlights the need for a well characterised set of standards in order to unify methods of measurement across the community working in this field.

The paper is organised as follows. In section 2 we describe the synthesis of our set of La(Fe,Si,Mn)H_δ samples and section 3 is devoted to the different experimental methods. In section 3.1 iso-field and isothermal magnetometry, and the derivation of entropy changes from such experiments is discussed. Heat capacity measurements are the subject of section 3.2, in which a bespoke Peltier cell DSC is compared with a commercial Quantum Design PPMS operated in relaxation mode. Section 3.3 looks at the estimation of ΔT_{ad} from either direct measurements or from the magnetic field-dependent heat capacity data presented in Section 3.2.

2. Materials Production

The MCP series of samples were produced using a powder metallurgical route. La-Fe-Mn-Si master alloys were crushed and milled to a fine powder using a jet mill under inert conditions. The particle size distribution was analyzed by laser diffraction and the mean particle sizes (d50 value) of about 6 µm were reached. Five different alloy compositions were produced by blending and mixing the according master alloys. Subsequently, green parts were obtained by isostatic pressing applying

pressure of 1.5 to 4 t.$(cm)^{-2}$. These parts were sintered at temperatures ranging from 1333 K to 1373 K for about 4h under inert conditions. After sintering the composition of the samples was determined by X-ray fluorescence analysis. Hydrogenation was carried out after the samples had been heated to 773 K in an argon atmosphere. At 773 K argon was replaced with hydrogen and the samples were cooled down to room temperature within about 10h. After hydrogenation the parts were milled to a particle size of 400 – 500 μm using a disc mill.

The entropy change of the complete series of La-Fe-Mn-Si samples described in Table 1 at a fixed field change of 1.2 T is shown in Fig. 1. For the purposes of this round robin review, we choose to show data from MCP1011 from across the different laboratories. A backscattered scanning electron image of the sample surface of MCP1011 is given in Fig. 2.

Sample	Composition	T_c
MCP/1009	$LaFe_{11.350}Mn_{0.390}Si_{1.26}H_{1.53}$	T_c~10˚C
MCP/1010	$LaFe_{11.367}Mn_{0.373}Si_{1.26}H_{1.54}$	T_c~13˚C
MCP/1011	$LaFe_{11.384}Mn_{0.356}Si_{1.26}H_{1.52}$	T_c~17˚C
MCP/1012	$LaFe_{11.402}Mn_{0.338}Si_{1.26}H_{1.52}$	T_c~ 20˚C
MCP/1013	$LaFe_{11.418}Mn_{0.322}Si_{1.26}H_{1.53}$	T_c ~23˚C

Table (1)- Summary of the La-Fe-Mn-Si samples shown in Fig. 1.

3. Experimental Methods and Results

3.1. Magnetometry

Most usually the magnetisation is measured isothermally as a function of magnetic field $M(H)$, as shown in Fig. 3, and the entropy change, $\Delta S(T)$, is determined numerically using the Maxwell relation by first constructing the $M(T)$ curves. The preference for using this step rather than directly measuring $M(T)$ in fixed field is that the temperature gradient which can be set up in the cooling process will mean that either the sample is not at the bath temperature (which can introduce errors) or the rate of cooling has to be very slow. Overall this can result in a more laborious methodology, but if care is taken both methods yield reliable results.

Fig. 3 shows the magnetisation curves taken on MCP1011 using commercial equipment in two laboratories (IC and IFW). Errors can be introduced if the magnetometers have not been set by a standard calibration sample (in these experiments a standard NIST Ni sphere was used); if the thermometry is not calibrated; if the sample mass is not known accurately; and if the sample shape introduces demagnetisation effects. The final source of error is magnetic field history, and this is particularly important for first-order materials with large hysteresis. Minor thermal or field hysteresis loops can leave the sample in a partially transformed state leading to erroneous $M(H)$ curves and incorrect $\Delta S(T)$ estimates.

In the example given below, the sample used in (a) was a small set of as prepared particles (of size 400 – 500 μm) held freely in a powder capsule, whereas in (b), the particles were glued and formed into a pellet shape. These are typical methods used for measuring brittle samples and are common procedure with magnetocaloric materials that undergo a large magneto-volume or structural transition. The saturation magnetisation captured in each experiment at high field (2 T) and 265 K agrees to within 2% accuracy, which is reasonable. Note that the data in (a) was obtained using a vibrating sample magnetometer where the sample is vibrated at 66 Hz, and the field is swept at 20 $mT.s^{-1}$. In (b), the data was taken using a SQUID magnetometer where it is necessary to wait for a settle time of a few seconds between field steps. The hysteresis that is observed in the $M(H)$ curves in (a) results in this case from the MCE effect itself, whereby large samples with low thermal conductivity or in conditions of less than ideal heat exchange heat up on the timescale of the measurement. Such extrinsic hysteresis can be eliminated by performing experiments at lower sweep rates, as in Fig. 3b, or smaller sample volume (Moore et al. 2009) .

Fig. 4a shows that either $M(T)$ curves can be measured directly (by VAC) or can be created indirectly by extraction from the $M(H)$ curves (shown previously in Fig. 3) and no significant error is introduced

either in the shape of the $M(T)$ curves or, as shown in Fig. 4b, from the resulting ΔS curves that are calculated from them using a standard Maxwell relation. The curves are in reasonable agreement. The discrepancy between the symbols and the solid curves relates to the fact that the indirect method produces discrete information only. Improvement can be made if smaller temperature intervals are chosen for $M(H)$ curves in the temperature range of interest, or if an interpolation method is used to produce smooth curves from the constructed $M(T)$. Error can be introduced when $M(H)$ curves are converted to $M(T)$ if the resulting data is noisy. This can produce anomalous spikes in the ΔS curve and unevenness or steps in the $\Delta S(T)$ curve shape, that are simply artefacts. Magnetometry is one of the most common laboratory techniques and as a result experimental artefacts are reasonably well understood. Aside from the potential introduction of extrinsic hysteresis (Moore et al. 2009) the variability between data taken in different laboratories introduces only marginal error.

3.2. Heat Capacity

Magnetocaloric characterisation of materials requires the measurement of the temperature dependence of either adiabatic temperature change ($\Delta T_{ad}(T)$) or isothermal entropy change ($\Delta S(T)$) associated with a certain magnetic field variation, ΔH. Both these quantities can be obtained by the knowledge of the entropy curves under magnetic field ($S(T,H)$) through, respectively, the iso-entropy and isothermal subtraction of the curves performed at different magnetic fields (Pecharsky et al. 2001). The experimental access to entropy can be achieved by integrating specific heat curves, therefore for magnetocaloric materials, the direct measure of the dependence of specific heat on magnetic field ($C_p(T,H)$) is as important as other direct measurements. Here we review some of the methods used to extract specific heat and show that even using commercial instrumentation can lead to significantly different results between laboratories. We point out some of the key methods and pitfalls.

Several calorimetric methods are used to determine the specific heat of substances, and commercial devices are available. However, the measure of specific heat under magnetic field can be more critical because relatively high magnetic field can be produced only over restricted volumes. The investigation of magnetocaloric effect has triggered the development of laboratory instrumentation for this purpose based on different calorimetric methods, for example: semiadiabatic heat pulse techniques (Pecharsky et al. 1997[b]); relaxation calorimetry (Bachmann et al. 1972) (adopted in the Quantum Design PPMS); and heat flux differential scanning calorimetry (DSC) (Jeppesen et al. 2008; Marcos et al. 2003; Plackowski et al. 2002). In the case of a material showing a first order magnetic transition, it is interesting to separate the heat capacity and the latent heat contributions. Most of the methods mentioned above will capture both heat capacity and latent heat simultaneously. If it is of interest to understand how strongly first order a system is, based on the magnitude and evolution of the latent heat with magnetic field, this can be done using a microcalorimetry method as detailed by (Minakov et al. 2005) and (Miyoshi et al. 2008). The method has been applied to study $LaFe_{13-x}Si_x$ (Morrison et al. 2010), $La(Fe_{0.88}Si_{1-x}Al_x)_{13}$ (Morrison et al. 2011[a]) and CoMnSi (Morrison et al. 2009).

The temperature scanning techniques presented by Bachmann et al. (1972), Plackowski et al. (2002) and Marcos et al. (2003) are based on the use of miniaturized thermoelectric modules (Peltier cells) as sensitive heat flux, *q*, sensors. In a temperature scan at rate $\dot{T}$, the specific heat can be determined by $C_p = q/m\dot{T}$, where *m* is the mass of the sample. At INRIM, a Peltier cell DSC similar to those cited above was specifically developed for magnetocaloric characterisation. The problem of heat diffusion in the calorimeter was studied and the compensation methods were defined for producing specific heat curves that are not affected by the time constants introduced by the heat capacity of the thermoelectric modules itself. The interesting temperature range for magnetocaloric characterisation is focused around room temperature because for applications the materials are optimised in that region. The calorimeter specifically used for the round robin at INRIM operates in

the range from ~243 K (-30 °C) to ~363 K (90 °C). While the upper bound is not crossable because thermoelectric modules could be irreversibly damaged, the lower limit depends only on how much it is possible to cool the thermal bath. A similar calorimeter was reproduced in a cryostat to reach liquid helium temperature.

The construction and operation details of the experimental setup, its calibration and many results have been presented recently (Basso et al. 2010). As in a commercial DSC, reference materials are used either for the determination of the calibration constant, S_p, (connecting the voltage measured at the ends of the Peltier cells to the heat flux traversing them), or the time constant, τ_p, governing the kinetics of the calorimeter. In the first case a standard sapphire sample was used whose specific heat is tabulated. For the latter case a material without any thermal hysteresis and a good magnetocaloric response is measured and the time constant is adjusted until any apparent thermal hysteresis in C_p disappears. In this specific case, the sample used was a La-Fe-Co-Si alloy whose magnetocaloric properties were at the centre of a previous round robin test, within the SSEEC consortium, on second-order materials. The procedure uses measurements of C_p under different temperature rates and the time constant was chosen as the one that makes all the different curves collapse onto the same limit curve that should be not affected by the kinetic error. Notice that the compensation of the cell kinetics requires an additional calibration step with respect other DSC apparatus, nevertheless, the payback is the substantial reduction of the systematic errors introduced by the time constants which affect scanning calorimetry.

The INRIM calorimeter can also operate under isothermal conditions. In this case the heat flux is due to the change of the applied magnetic field and the induced entropy change is directly determined. In the temperature scanning regime, the setup was validated in the absence of a magnetic field by comparing its results with a commercial Perkin-Elmer Diamond^{TM} heat-flux compensation DSC. The measurement technique was demonstrated to be reliable and accurate and the corrections on

kinetics allowed the determination of the entropy curves from measurement under temperature scans performed at different scanning rates or with complex time sequences of temperature ramps. The kinetic correction appears to be practically indispensable for the characterisation of materials presenting the giant magnetocaloric effect. In this case the main effect of the magnetic field is the shift of the phase transition temperature, thus the kinetic correction allows a more accurate characterisation by removing any apparent temperature shift of the specific heat peaks due to instrumental effects. Peltier cell-based DSC looks to be either a laboratory instrument for fundamental studies on materials or a routine characterisation tool that can be potentially automated in any of its operations. At INRIM, it was largely employed for characterisation of the materials of the SSEEC project; study of spin reorientation for magnetic refrigeration (Basso et al. 2011); and the characterisation of different Heusler alloys presenting a first order magneto-structural phase transition (Ni-Mn-Sn (Plackowski et al. 2002), Ni-Fe-Ga (Basso et al. 2009), Ni-Mn-Ga (Sasso et al. 2008, 2011)).

In Fig. 5a the specific heat of MCP1011 measured under different applied magnetic fields is shown. In order to have a good signal to noise ratio, a sample with mass greater than 10-50 mg must be used in the calorimeter. Due to the granular nature of the sample, of particle size 4-500 µm, it was necessary to use a sample holder to host the powder. The powder was not compacted and the sample holder was a 5 mm diameter aluminium pan as provided by Perkin-Elmer for their DSC. The mass of the powder in the holder was 109.95 mg and the pan containing the powder was placed in contact to the thermoelectric cell upper surface with a small layer of thermal conductive paste (silver paste) in order to maximize the thermal contact. The use of a container for the sample and the undefined grade of thermal contact among the powder particles introduces additional uncertainty in the measurement process as any thermal contact accounts for a new thermal lag. In this case, however, the thermal lag due to the container was taken into account by including it in the

determination of the time constants of the calorimeter, whereas any lack of thermal homogeneity inside the granular sample was not taken into account.

All of the measurements were performed at a scanning rate of 2.5 K min^{-1}. This rate was chosen in order to either avoid any dynamical effects on the phase transition that cannot be excluded, or to be sure that the compensation of the time constants of the calorimeter is as good as possible. The control of the temperature rate was performed to within 1% by a digital Proportional-Integral-Differential (PID) controller.

In the relaxation method employed by QD PPMS, the sample is first heated above the bath temperature, T_b, to $T=T_b+\Delta T_{rise}$ by application of constant heating power, P. The temperature of the platform is then monitored as P is reduced to zero and the sample relaxes again to T_b via a weak thermal link. The heat capacity is determined by iterative fitting to the heat transfer equations described by Hwang et al. (1997). The universal disadvantages of relaxation calorimetry in the case of first order phase transitions or sharp second order phase transitions are explained by various authors (Hardy et al. 2009; Kennedy et al. 2007; Lashley et al. 2003; Morrison et al. 2011[b]; Suzuki et al. 2010). In this measurement technique incorrect measurement of C_p can occur at the phase transition if the specific heat is not constant over the temperature range imposed by the relaxation measurement (ΔT_{rise}). Deviation of temperature from the assumed exponential relaxation fails under the fitting algorithm of the PPMS and unpredictable and incorrect results will be provided. Separate analysis by examining the entire relaxation curves, as outlined by Lashley et al. (2003), and further developed by Suzuki et al. (2010) can however recover the full detail of the phase transition if the measurement parameters have been set correctly (Morrison et al. 2011[b]).

Comparison between the measurements performed by relaxation calorimetry used in the commercial PPMS (IFW-pellet of 2.5 mm diameter, < 0.5 mm thickness, and IC-free fragments) and

the temperature scanning method (INRIM –free fragments), are shown in Fig. 5b. The comparison shows several discrepancies.

The offset of the peak between the IC (PPMS) and the INRIM (DSC) is due to a thermometry calibration error. In fact, the temperature provided by the PPMS is that of the platform which the sample is attached to and not directly that of the sample itself, so this is the likely source of the error. In the case of a first-order phase transition, these two temperatures can be significantly different (in principle the temperature of the sample should remain constant during the first order phase transition). In the INRIM calorimeter, the lag between the measured temperature (that of the thermal bath) and the sample temperature was properly taken into account and partially corrected, as explained elsewhere (Basso et al. 2010)

The difference in the general shape of the two PPMS results can be explained by a number of possible factors. Firstly there is the spread in sample properties that can result from the pressing process used. Secondly, the apparent heat capacity curve can be broadened if the temperature rise used, ΔT_{rise}, is too large. This will result in a measurement that will average or smooth out features as the curve fitting method employed can only give an average over the temperature span (ΔT_{rise}). When the ΔT_{rise} of the IC data is artificially increased by averaging data points over a larger temperature window, it closely resembles the data taken at IFW on the pellet, as shown in Fig. 6. The third possible source of error is that for large samples with poor thermal conductivity the heat capacity can be underestimated if the temperature rise, ΔT_{rise}, is too large. This problem was demonstrated by Kennedy et al. (2007) using measurements of zirconium tungstate. We are also aware that the standard PPMS heat capacity puck is below the homogeneous field of the magnet and this can introduce further discrepancies but do not discuss it here as the comparative data shown in figure 5(b) are all taken in zero field.

3.3. Direct and Indirect Delta T (IFW)

The adiabatic temperature change ΔT_{ad} is a critical parameter to determine whether or not a magnetic material is attractive for magnetic cooling application. The term "direct method" refers to measurement of the sample temperature change by thermometry while indirect method refers to ΔT_{ad} obtained by other means, such as the measurement of heat capacity in zero and finite applied field. The indirect method is fairly common as calorimeters are commercially available and we have addressed the reliability of calorimeter measurements in the previous section. Direct ΔT_{ad} measurements on the other hand, are usually performed in a home-built experimental setup due to their lack of commercial availability. Several laboratories now report direct ΔT_{ad} measurements; in our case the set up is in IFW. As part of the round-robin exercise we compared the direct ΔT_{ad} (IFW) and indirect ΔT_{ad} (INRIM) for the MCP1011 sample. We highlight important parts of the IFW set-up and three main sources of error that can occur in direct ΔT_{ad} measurements.

In the experimental setup the magnetic field was produced by permanent magnets arranged in two Halbach cylinders, one contained within the other and having a central bore for the sample space. By rotating one cylinder with respect to the other, H could be changed from 0 to 1.93 T at a rate of up to 2 $T.s^{-1}$. The sample temperature change was monitored continuously as a function of field, $\Delta T_{ad}(H)$, with accuracy better than ±0.01 K by a copper-constantan thermocouple, while the sample was insulated by a series of passive heat shields and kept under vacuum conditions. This highlights the first source of error in ΔT_{ad} due to non-adiabatic conditions, i.e. heat loss from the sample to the environment. We performed a simple test to confirm adiabatic conditions in our setup by measuring $\Delta T_{ad}(H)$ for the second-order transition in Gd, which showed no hysteresis (within error) as expected for a reversible adiabatic process. Other sources of irreversibility, such as eddy current heating and motion of domain walls, can be neglected in the case of Gd near its T_c (293 K).

Fig. 7 compares $\Delta T_{ad}(T)$ measured with direct and indirect methods for MCP1011. The curves are shown for a field change of 0.4, 0.8, and 1.2 T where the starting field value was zero. The two methods show good agreement between the $\Delta T_{ad}(T)$ curves, except we see that there is a discrepancy of the order of 10% in the peak ΔT_{ad} value. One potential reason for this could be the demagnetisation factor associated with the sample geometry. This effect has been discussed recently and it is important to note that it still has such a significant effect at high fields (Kuz'min et al. 2011). This brings us to the next source of error to consider, which is how the sample is prepared for measurement and its shape. In our case, the MCP1011 sample was a powder. Direct ΔT_{ad} measurement requires approximately 1 g of material and the powder must be mechanically pressed into a pellet (of dimensions 1x5x10 mm) to enable a reliable measurement. At this point the thermocouple can be placed inside the pellet, greatly improving the thermal contact between sample and thermocouple. The field was changed at a slower rate of 0.5 $T.s^{-1}$ to enable thermal equilibrium to be reached within the sample, while the measurement conditions still remained adiabatic-like. Using the method of Kuz'min *et al*. (2011) the direct and indirect ΔT_{ad} curves could be corrected for demagnetisation effects, which for H = 1.2 T would correspond to *at most* a 6% increase in the direct data with respect to the indirect data and so does not account for the full discrepancy. It is possible however that the process of pressing the pellet broadened the phase transition as was observed in the calorimetry measurements of section 3.2.

The final source of error we consider is due to the measurement protocol used when the transition being studied is first-order. The presence of superheating or supercooling means that the sample pre-history can affect the magnitude of ΔT_{ad} (Skokov et al. 2011). Measurements are said to be done on *warming* protocol when going from low to high temperature in discrete ΔT steps, or on *cooling* protocol when in the reverse direction from high to low temperature in steps. In the case of cooling protocol near to T_c the sample can be prepared in a supercooled paramagnetic state leading to a maximum ΔT_{ad} when it is first magnetised. In contrast, on heating protocol the sample can be

superheated, which leads to a reduced ΔT_{ad}. Therefore it is important to specify the protocol used and ideally ΔT_{ad} should be measured using both protocols (Sasso et al., 2008).

Under repeated cyclic action of H, such as in a real cooling device, it is the warming curve that determines the ΔT_{ad} achieved in practice (Skokov et al. 2011) and it is exactly this data which is most useful for application. In Fig. 7 we show direct ΔT_{ad} measured under both protocols (open and closed symbols). The two curves almost coincide, which shows that the warming curve is not suppressed in the MCP1011 sample. The reason is the small thermal hysteresis (1 K) in the MCP1011 sample. In this regard the La-Fe-Mn-Si-H alloys perform very well and it highlights the need for small hysteresis in a magnetocaloric material.

4. Conclusions

We have shown the variance in experimental measurement of the $M(H,T)$, $C_p(H,T)$, ΔS, ΔT_{ad} in different laboratories demonstrating how sample geometry and field history are paramount and that standards must be used to calibrate thermometry and magnetometry. No such standards exist for direct ΔT_{ad} measurements or heat capacity, although samples of known performance can be used. For an informative comparison of data across different laboratories it is of paramount importance for several key factors of the experimental protocol to be made clear. This includes but is not limited to a) measurement parameters such as field sweep rate or the ΔT_{rise} used in commercial heat capacity measurements; and b) sample preparation and form, such as geometry (and field alignment with respect to this), whether the sample is glued or held freely, or whether a powder was pressed into a pellet.

5. Acknowledgements

The research leading to these results has received funding from the European Community's 7th Framework Programme under grant agreement no. 214864 ("SSEEC"). K.G.S. acknowledges financial support from The Royal Society.

References

Bachmann, R., Schwall, R.E., Thomas, H.U., Zubeck, R.B., King, C.N., Kirsch, H.C., Disalvo, F.J., Geballe, T.H., Lee, K.N., Howard, R.E., and Greene, R.L., 1972. Heat-Capacity Measurements on Small Samples at Low-Temperatures. Rev. Sci. Instrum. 43, 205-214.

Basso, V., Balma, D., Sasso, C.P., Küpferling, M., Vasiliev, A., and Chumlyakov, Y., 2009. Thermomagnetic properties of single crystal Ni(54)Fe(19)Ga(27) Heusler alloys. J. Appl. Phys. 105, 07A937.

Basso, V., Sasso, C.P., and Küpferling, M. 2010. A peltier cells differential calorimeter with kinetic correction for the measurement of $c_p(H,T)$ and $\Delta S(H,T)$ of magnetocaloric materials. Rev. Sci. Instrum. 81, 113904.

Basso, V., Sasso, C.P., Kupferling, M., Skokov, K.P., and Gutfleisch, O., 2011. Er(2)Fe(14)B single crystal as magnetic refrigerant at the spin reorientation transition. J. Appl. Phys. 109, 083910.

Fujita, A., Fujieda, S., Hasegawa, Y., and Fukamichi, K., 2003. Itinerant-electron metamagnetic transition and large magnetocaloric effects in La(Fe(x)Si(1-x))(13) compounds and their hydrides. Phys. Rev. B 67, 104416.

Gschneidner, K. A. and Pecharsky, V.K., 2000. Magnetocaloric materials. Ann. Rev. Mater. Sci. 30, 387-429.

Gschneidner, K. A., Pecharsky, V.K., and Tsokol, A.O., 2005. Recent developments in magnetocaloric materials. Rep. Prog. Phys. 68, 1479-1539.

Gutfleisch, O., Willard, M.A., Bruck, E., Chen, C.H., Sankar, S.G., and Liu, J.P., 2011. Magnetic materials and devices for the 21st century: stronger, lighter, and more energy efficient. *Adv. Mater.* 23, 821-842

Hardy, V., Breard, Y. and Martin, C., 2009. Derivation of the heat capacity anomaly at a first-order transition by using a semi-adiabatic relaxation technique. J. Phys.: Condens. Matter 21,075406.

Hu, F. X., Gao, J., Qian, X.L., Ilyn, M., Tishin, A.M., Sun, J.R., and Shen, B.G., 2005. Magnetocaloric effect in itinerant electron metamagnetic systems La(Fe(1-x)Co(x))(11.9)Si(1.1). J. Appl. Phys. 97, 10M303.

Humphries, M. 2010. Rare earth elements: The global supply chain. CRS Report for Congress, R41347 (Congressional Research Service, Library of Congress)
http://www.fas.org/sgp/crs/natsec/R41347.pdf

Hwang, J. S., Lin, K.J., and Tien, C., 1997. Measurement of heat capacity by fitting the whole temperature response of a heat pulse calorimeter. Rev. Sci. Instrum. 68, 94.

Jeppesen, S.,Linderoth, S., Pryds, N., Kuhn, L.T., and Jensen, J.B., 2008. Indirect measurement of the magnetocaloric effect using a novel differential scanning calorimeter with magnetic field. Rev. Sci. Instrum. 79, 083901.

Kennedy, C. A., Stancescu, M., Marriot, R.A., and White, M.A., 2007. Recommendations for accurate heat capacity measurements using a Quantum Design physical property measurement system. Cryogenics 47, 107-112.

Kuz'min, M. D., Skokov, K.P., Karpenkov, D.Y., Moore, J.D., Richter, M., and Gutfleisch, O., 2011. Magnetic field dependence of the maximum adiabatic temperature change.Appl. Phys. Lett. 99, 012501.

Lashley, J. C., Hundley, M.F., Migliori, A., Sarrao, J.L., Pagliuso, P.G., Darling, T.W., Jaime, M., Cooley, J.C., Hults, W.L., Morales, L., Thoma, D.J., Smith, J.L., Boerio-Goates, J., Woodfield, B.R., Stewart, G.R., Fisher, R.A., and Phillips, N.E., 2003. Critical exmination of heat capacity measurements made on a Quantum Design physical property measurement system. Cryogenics 43, 369-378.

Lyubina, J., Gutfleisch, O., Kuz'min, M., and Richter, M. 2008. La(Fe,Si)(13)-based magnetic refrigerants obtained by novel processing routes. J. Magn. Magn. Mater. 320, 2252.

Marcos, J., Casanova, F., Batlle, X., Labarta, A., and Planes, A., 2003. A high-sensitivity differential scanning calorimeter with magnetic field for magnetostructural transitions. Rev. Sci. Instrum. 74, 4768.

Minakov, A. A., Roy, S.B., Bugoslavsky, Y.V., and Cohen, L.F., 2005. Thin-film alternating current nanocalorimeter for low temperatures and high magnetic fields. Rev. Sci. Instrum. 76, 043906.

Miyoshi, Y., Morrison, K., Moore, J.D., Caplin, A.D., and Cohen, L.F., 2008. Heat capacity and latent heat measurements of CoMnSi using a microcalorimeter. Rev. Sci. Instrum. 79, 074901.

Moore, J. D., Morrison, K., Sandeman, K.G., Katter, M., and Cohen, L.F., 2009. Reducing extrinsic hysteresis in first-order La(Fe,Co,Si)(13) magnetocaloric systems. Appl. Phys. Lett. 95, 252504.

Morrison, K., Podgornykh, S.M., Shcherbakova, Y.V., Caplin, A.D., and Cohen, L.F., 2011[a]. Effect of Al substitution on the magnetocaloric properties of La(Fe(0.88)Si(0.12-x)Al(x))(13). Phys. Rev. B 83, 144415.

Morrison, K., 2011[b]. "Preprint."

Morrison, K., Lyubina, J., Moore, J.D., Caplin, A.D., Sandeman, K.G., Gutfleisch, O., and Cohen, L.F., 2010. Contributions to the entropy change in melt-spun LaFe(11.6)Si(1.4). J. Phys. D:Appl. Phys. 43, 132001.

Morrison, K., Moore, J.D., Sandeman, K.G., Caplin, A.D., and Cohen, L.F., 2009. Capturing first- and second-order behavior in magnetocaloric CoMnSi(0.92)Ge(0.08). Phys. Rev. B 79, 134408.

Pecharsky, V.K., Gschneidner, K.A., Jr., Pecharsky, A.O., and Tishin, A.M., 2001. Thermodynamics of the magnetocaloric effect. Phys. Rev. B 64, 144406.

Pecharsky, V.K., and Gschneidner, K.A., 1997[a]. Giant magnetocaloric effect in Gd-5(Si2Ge2). Phys. Rev. Lett. 78, 4494-4497.

Pecharsky, V.K., Moorman, J.O., and Gschneidner, K.A. 1997[b]. A 3-350 K fast automatic small sample calorimeter. Rev. Sci. Instrum. 68, 4196-4207.

Plackowski, T., Yuxing, W., and Alain, J., 2002. Specific heat and magnetocaloric effect measurements using commercial heat-flow sensors. Rev. Sci. Instrum. 73, 2755-2765.

Sandeman, K.G., 2011. Gas-free Refrigeration. Magnetics Technology International 1, 32.

Sasso, C. P., Zheng, P.Q., Basso, V., Mullner, P., and Dunand, D.C., 2011. Enhanced field induced martensitic phase transition and magnetocaloric effect in Ni(55)Mn(20)Ga(25) metallic foams. Intermetallics 19, 952-956.

Sasso, C.P., Küpferling, M., Giudici, L., Basso, V., Pasquale, M., 2008. Direct measurements of the entropy change and its history dependence in Ni-Mn-Ga alloys. J. Appl. Phys. 103, 07B306

Schüler, D., Buchert, M., Liu, R., Dittrich, S., and Merz, C., 2011. Study on Rare Earths and Their Recycling, Darmstadt, Oeko-Institut., http://www.oeko.de/oekodoc/1112/2011-003-en.pdf

Skokov, K. P., Khovaylo, V.V., Mueller, K.-H., Moore, J. D., Liu, J., and Gutfleisch, O., 2011. Magnetocaloric materials with first-order phase transition: thermal and magnetic hysteresis in LaFe11.8Si1.2. submitted to J. Appl. Phys..

Suzuki, H., Inaba, A., and Meingast, C., 2010. Accurate heat capacity data at phase transitions from relaxation calorimetry. Cryogenics 50, 693-699.

Tassou, S. A., Lewis, J., Ge, Y.T., Hadawey, A., and Chae, I., 2010. A review of emerging technologies for food refrigeration applications. Appl. Therm. Eng. 30, 263-276.

Tegus, O., Bruck, E., Buschow, K.H.J., and de Boer, F.R., 2002. Transition-metal-based magnetic refrigerants for room-temperature applications. Nature 415, 150-152.

Yan, A., Müller, K.-H. and Gutfleisch, O., 2005. J. Appl. Phys. 97, 036102.

Figures

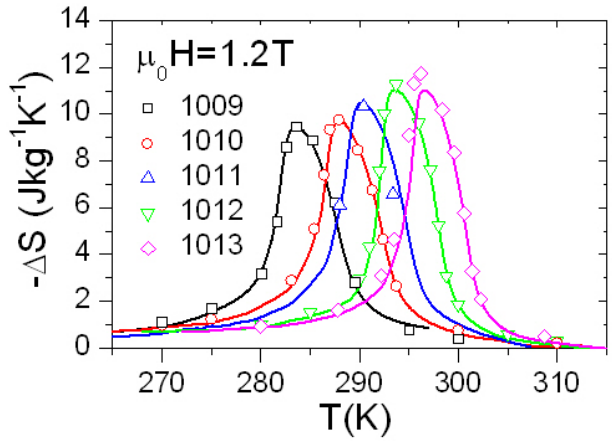

Fig. 1 – Entropy change measured by INRIM for the complete series of La-Fe-Mn-Si samples described in Table 1 for a fixed field change of 0 - 1.2 T (colour online).

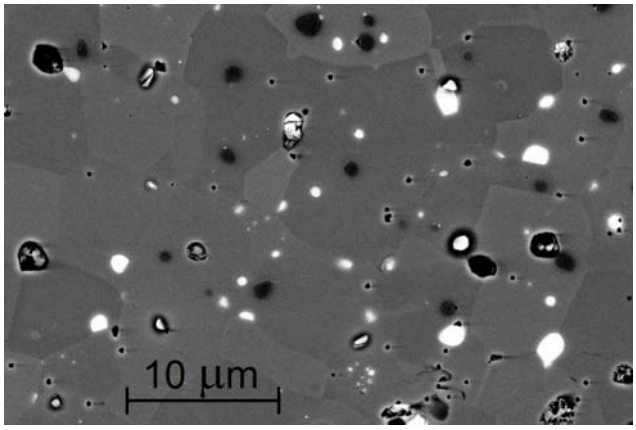

Fig. 2 – Backscattered scanning electron microscope image of the MCP1011 alloy. Black areas indicate alpha-Fe; grey $LaFe_{11.384}Mn_{0.356}Si_{1.26}H_{1.52}$; and white is La-rich phase.

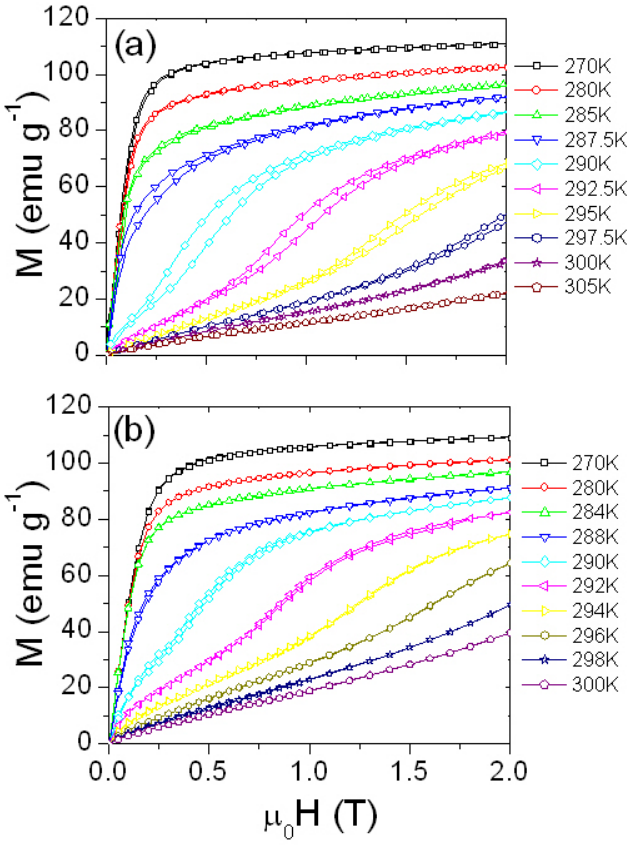

Fig. 3 - Magnetisation versus applied field for the MCP1011 sample (colour online). Data taken at (a) Imperial College (IC) using an Oxford Instruments vibrating sample magnetometer, (saturation magnetisation 112 emu.g^{-1} at 265 K and 2 T) and (b) IFW using a PPMS SQUID magnetometer (saturation magnetisation 110 emu.g^{-1} at 265K and 2 T).

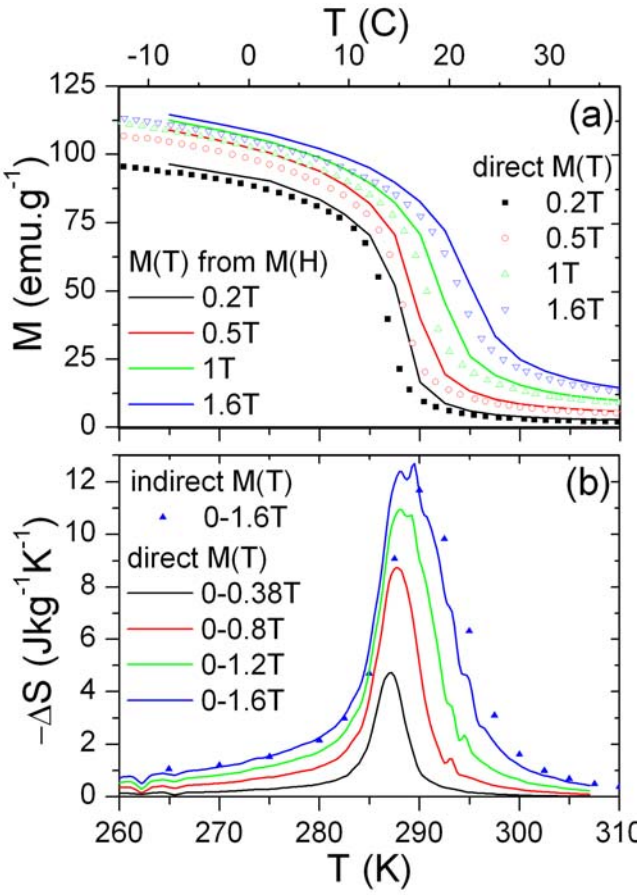

Fig. 4 - Entropy change determined from magnetisation measurements (colour online). (a) $M(T)$ curves measured directly (VAC) and extracted from $M(H)$ curves (IC/IFW). (b) The entropy change ΔS calculated from the $M(T)$ curves shown in (a).

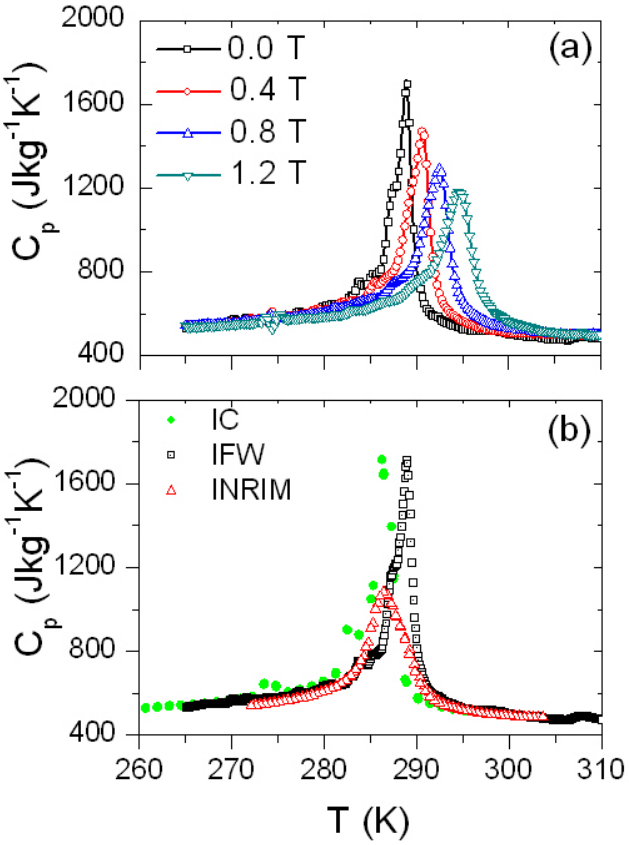

Fig. 5 – Heat capacity data for the MCP1011 sample (colour online). (a) INRIM data taken in various fixed external fields, and (b) heat capacity in zero field: a comparison of heat capacity taken in three laboratory environments using different methods.

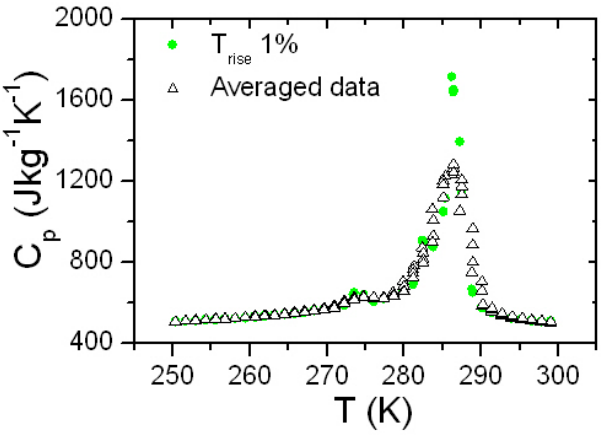

Fig. 6 – Impact of experimental parameters on PPMS measurements (colour online). Graph shows the result of averaging heat capacity over a large temperature window (~2%T_{bath}) where the sharp change in heat capacity now resembles broad behaviour observed in the pellet.

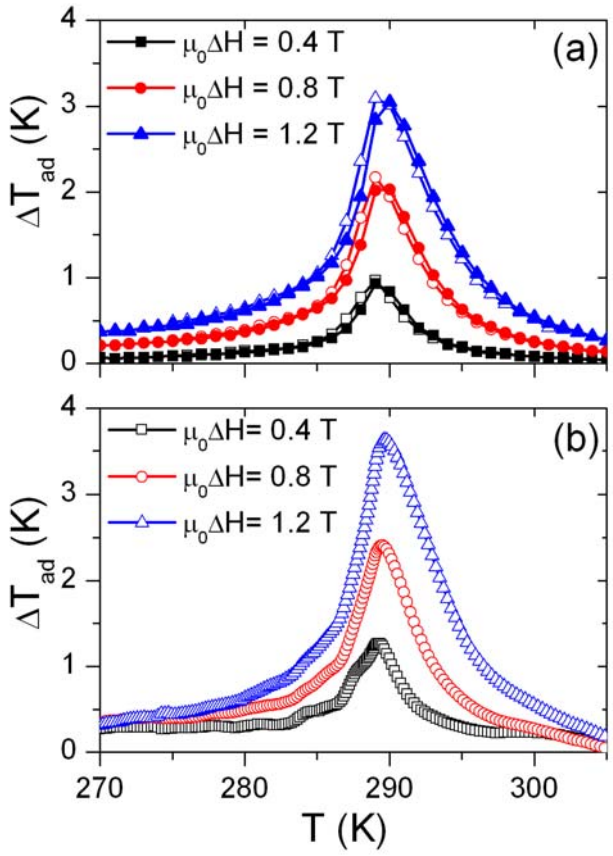

Fig. 7 – Adiabatic temperature change for MCP1011 in the constant applied fields 0.4, 0.8, and 1.2 T (colour online). (a) Direct ΔT_{ad} curves from IFW under cooling protocol (open symbol) and warming protocol (closed symbol), and (b) indirect ΔT_{ad} from INRIM calculated from the entropy change and the heat capacity.